Available online at www.sciencedirect.com

SCIENCE DIRECT®

Polymer 45 (2004) 2657–2663

polymer

www.elsevier.com/locate/polymer

Comparison of methods for characterizing comonomer composition in ethylene 1-olefin copolymers: 3D-TREF vs. SEC-FTIR

Chung C. Tso*, Paul J. DesLauriers

Chevron Phillips Chemical Company LP, Bartlesville, OK 74004, USA

Received 20 November 2003; received in revised form 21 January 2004; accepted 23 January 2004

Abstract

In this paper, two methodologies for determining comonomer composition in ethylene 1-olefin copolymers, namely three detectors coupled to a temperature rising elution fractionation unit (3D-TREF) and size exclusion chromatography coupled to a Fourier transfer infrared detector (SEC-FTIR), are examined and compared. Because the two methods are based on different separation mechanisms, insight into the resin's molecular architecture is gained from two entirely different, yet complementary perspectives. The choice of which method to use will be determined by the specific structure vs. property issue under study. Comparative results from the analysis of copolymers produced by Ziegler–Natta, chromium and metallocene catalysts show that both the methods are useful for characterizing LLDPE resins. However, the 3D-TREF method may offer more insight into the heterogeneity of resin blends, particularly when the blend components have similar molecular weights. Although some MW-dependency information of the temperature fractions can be ascertained via viscometer and light scattering detectors, SEC-FTIR is the more appropriate method to detect compositional heterogeneity in resin blends that are composed of two or more resins with the same copolymer compositions, but with different molecular weights.

Keywords: Ethylene copolymers; Short chain branching techniques; Comonomer composition

1. Introduction

With the ever-increasing compositional heterogeneity of ethylene 1-olefin copolymers and/or blends, the knowledge of simply the MW/MWD of a resin, available from the size exclusion chromatograph, is no longer sufficient to define the architecture of the resin. It is well accepted that the density of the resin, which was achieved most effectively via the incorporation of comonomers into the polymer chain, plays an equally important role in determining the resin performance properties. However, depending upon the kind of catalyst, reactor processing technology and conditions involved in the manufacturing process, resins of similar density might exhibit significant differences in comonomer content and distribution, at both the inter-molecular and intra-molecular levels. In turn, these differences at the molecular level will result in pronounced differences in resin performance properties such as impact strength, stress crack resistance, hot tack, heat seal and hexane extractables, to name just a few [1,5,9,14,15]. For this reason, considerable effort has been made in recent years to develop analytical techniques that characterize the chemical composition distribution of the resin in a timely fashion.

In this paper, we describe and compare two methods for the analysis of the comonomer content and distribution in PE copolymers. The size exclusion chromatography coupled to a Fourier transfer infrared detector (SEC-FTIR) method separates polymer molecules by their size and utilizes FTIR to measure the average comonomer content within a narrow slice of the resin's molecular weight distribution (MWD) [2–5]. Overall, this method generates a comonomer distribution profile across the MWD of the resin. The other method, namely, three detectors coupled to a temperature rising elution fractionation unit (3D-TREF), separates polymer molecules by their crystallization temperature (the mechanism for temperature rising elution fractionation or TREF) [4,6–13]. Furthermore, by adding MW-sensitive viscometer and light scattering (LS) detectors to the typical infrared (IR) concentration detector, some MW information for the fractions of different comonomer content within the resin can be obtained [16,17]. TREF systems with these three detectors (IR, viscosity and LS) are referred to as 3D-TREF units.

---

* Corresponding author. Tel.: +1-918-661-4766; fax: +1-918-662-6072.
E-mail address: tsocc@cpchem.com (C.C. Tso).

0032-3861/$ - see front matter © 2004 Elsevier Ltd. All rights reserved.
doi:10.1016/j.polymer.2004.01.066

The purpose of this paper is to give the reader an appreciation for both the advantages and limitations inherent in each methodology. Samples produced by different catalysts will be used to illustrate the molecular structural features revealed by the two methods.

2. Experimental

The SEC-FTIR instrument in essence adds the FTIR detector to the standard SEC unit to measure the average comonomer content of each fraction of narrow MWD separated by their size inside the column packed with porous beads. Polyethylene molecules in hot 1,2,4-trichlorobenzene (TCB) are carried downstream through the column. The larger molecules do not penetrate much into the pores of the packing beads and elute first, followed by the smaller molecules. The FTIR detector serves both as a SEC concentration detector used for the measurement of MW and as a means by which the comonomer content of the eluting molecules is determined. More details of the SEC-FTIR instrument assembly and methodology to determine SCB can be found in the publication references [5].

The 3D-TREF instrument has been assembled using parts retro-fitted into a Waters 150C GPC/SEC system. A schematic view of the components of the assembly can be found in a previous publication [16,17]. A TREF column (0.5 in. ID and 6 in. in length) packed with #30 SS shots (Vulcan Blast Shot Technology, Brantfor, Ontario Canada) was used. The TREF oven heater, which provides programmed cooling (from 150 to 35 °C) and heating (from 35 to 150 °C) to the column during the experiment, was controlled externally via West 4400 set point programmer. The three detectors used were a Foxboro IR (3.4 nm), a Viscotek 150R viscometer and a PDI 15 and 90-degree dual-angle LS detector. The viscometer and the LS detector were housed in the same oven while the IR cell was heated separately. 1,2,4-Trichlorobenzene (TCB) was used as the carrier solvent at 0.5 ml/min flow rate. A 3 mg/ml sample concentration with a 500 μl injection volume was used. The data reported in this paper were taken with a four-hour run time for each sample. All detector response plots were normalized by area.

Like the instrumentation assembly, a graphic illustration of the separation mechanism of the TREF operation can also be found in the same publication [16,17]. In the experiment, a sample solution is injected and held inside the column and subsequently cooled. During the cooling step, polymer molecules are allowed to crystallize and form layer upon layer of coating on the packing particles. The column is then heated, during which time the polymer molecules are re-melted and re-dissolved into the solvent flow stream and elute out. Polymer molecules with higher comonomer content elute from the column first at lower elution temperature. Concentration and the molecular weight information of the polymer molecules at each individual temperature as they emerge from the TREF column are obtained using the three-detector array. The IR detector signal is proportional to sample concentration only. Whereas the viscometer and LS detector signals, when coupled to the IR detector are not only proportional to the concentration, but are also proportional to the polymer intrinsic viscosity (IV) and MW, respectively.

Table 1
Polyethylene samples

Sample ID	Density (g/cm^3)	MI	M_w (kg/mol)	M_n (kg/mol)	PDI	Mole % (H)
ZN-1	0.9184	0.90	138	28.5	4.9	4.0
ZN-2	0.9170	0.85	138	27.9	4.9	4.0
ZN-3	0.9160	0.85	145	31.2	4.6	4.1
ZN-4	0.9170	0.50	160	38.0	4.2	3.7
ZN-5	0.9208	0.50	136	26.8	5.1	3.2
ZN-6	0.9246	0.50	139	21.4	6.5	2.5
Cr-1	0.9230	0.25	201	16.5	12.2	NA
Cr-2	0.9370	0.30	209	11.8	17.7	NA
MET-1	0.8960	2.60	111	63.3	1.7	6.9
MET-2	0.9180	1.00	101	43.8	2.3	2.3
MET-3	0.9180	1.00	101	43.8	2.3	2.3
MET-4	0.9170	0.85				2.7
MET-5	0.9170	0.77	113	40.2	2.8	2.7
MET-6	0.9330	1.00	105	37.5	2.8	0.6
MET-7	0.9343	7.40				1.9
MET-8	0.9199	0.46	155	22.4	6.9	3.3
MET-9						NA

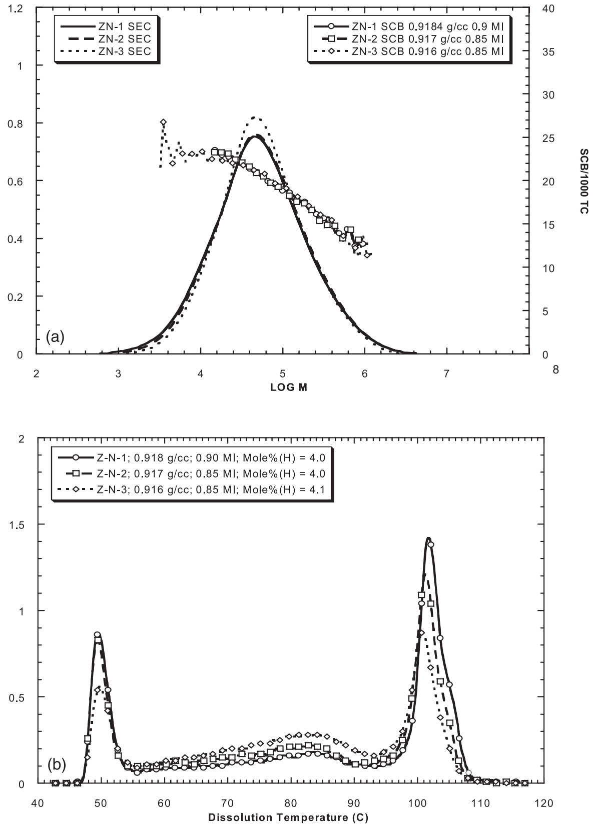

Fig. 1. (a) SEC-FTIR Profiles of Z–N samples of comparable density and MI. (b) TREF profiles of Z–N samples of comparable density and MI.

The density, MI and other molecular characterization data of the samples are documented in Table 1.

3. Results and discussion

3.1. Ziegler–Natta catalyzed resins

The SEC-FTIR profiles of three E/H copolymer samples of similar density and MIs produced by three different Ziegler–Natta catalysts are dipicted in Fig. 1(a). ^{13}C NMR analysis also shows these samples have approximately the same comonomer content. The average comonomer content distribution profiles across the MWD of the three samples are almost indistinguishable in their SCB frequency. As shown in Fig. 1(a), the comonomer content in these resins varies from high to low across the MWD. This is typically observed for resins of this density produced using a Ziegler–Natta catalyst.

By comparison, the TREF plots shown in Fig. 1(b) reveal that the three samples share some common features but also show pronounced differences. All three samples possess the comonomer composition profile characteristic of the resins produced by Ziegler–Natta catalyst. Each individual profile is composed of three fractions. First, a soluble fraction elutes out between 45 and 55 °C, which is heavily concentrated with comonomers. Secondly, a linear homopolymer fraction with little and/or no comonomer elutes out at 95 °C or above. Thirdly, an in-between so-called ‘branched’ fraction is made up of polymer molecules of various comonomer content whose elution temperature covers a broad range of roughly 40°. The profiles all start around 45 °C and finish around 113 °C.

However, the relative amount of the three fractions within each individual sample varies appreciably. Sample ZN-1 has highest amounts of both the soluble and the linear homopolymer fractions, followed by sample ZN-2 and ZN-3 in decreasing order. Also of note is the peak dissolution temperature of the linear homopolymer fraction of sample A, which is slightly higher than the other two samples. It is also interesting to note that although all three-parent samples are of similar density, MI and comonomer content, the amount of soluble fraction in these samples significantly varies. These data suggest that sample ZN-3 has a more overall homogeneous comonomer composition distribution profile than samples ZN-1 and ZN-2.

In Fig. 2(a), the SEC-FTIR profiles of three copolymer samples of similar MIs but with different densities are

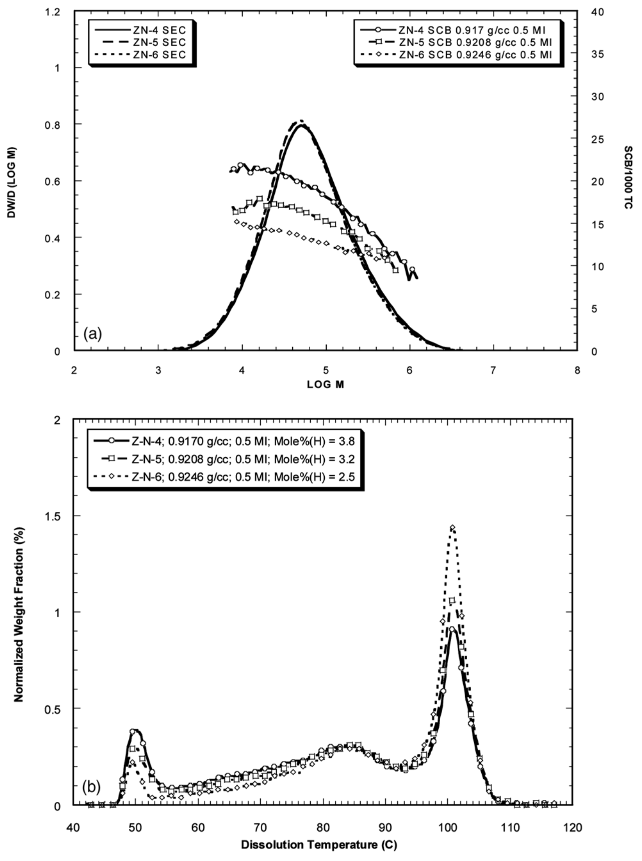

Fig. 2. (a) SEC-FTIR Profiles of Z–N samples of different density. (b) TREF profiles of Z–N samples of different density but comparable MI.

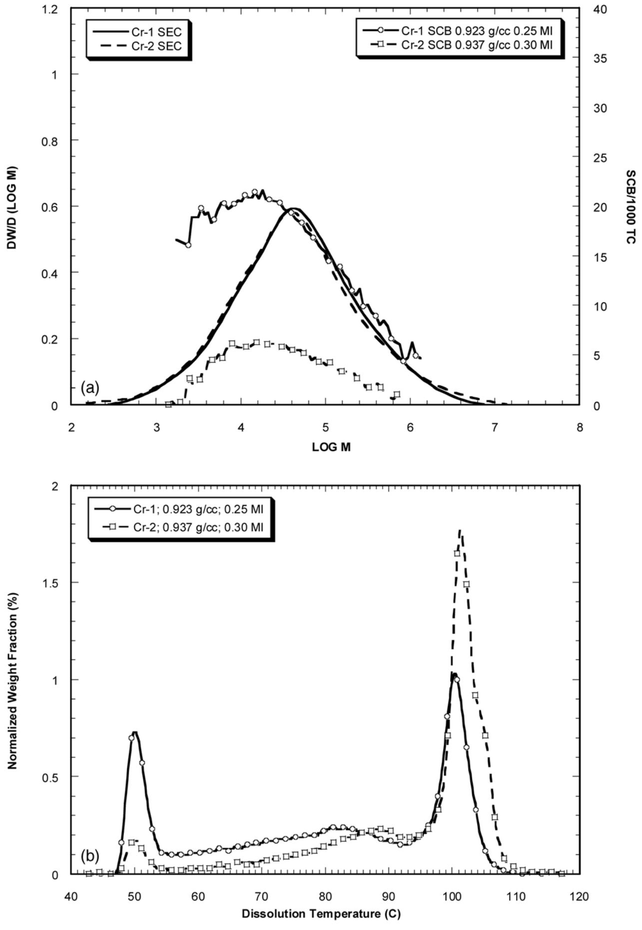

Fig. 3. (a) SEC-FTIR profiles of chrome samples of different density. (b) TREF profiles of chrome samples of different density.

compared. First, the profiles clearly show the same trend regarding the comonomer content distribution vs. MWD profiles, i.e. more comonomers at the low MW end and less at the high MW end. Secondly, they show the amount of comonomer content of each individual sample is inversely proportional to the density of the resin. Thirdly, the profiles all converge at the high MW end of the MWD but are much further apart at the low MW end. Also, their individual SCB frequency at the low MW end is significantly different from one another. Clearly, the SCB frequency vs. MWD of sample ZN-4 of 0.917 g/cm^3 shows the steepest and most curvaceous rise toward the low MW end. This suggests the comonomer goes preferentially to the low MW end of the MWD as resin density decreases.

The TREF plots in Fig. 2(b) of the three samples also show the comonomer composition distribution profiles typical of the Ziegler–Natta based resins. However, the relative amount of the constituent fractions among the three samples is quite different. As the density decreases, the amounts of the soluble as well as the branched fractions increase considerably while the linear homopolymer fraction decreases. However, the overall elution temperature range from start to finish is again the same.

3.2. Chromium catalyzed resins

Fig. 3(a) depicts the SEC-FTIR results of two chromium-based samples of varying density. Their profiles closely resemble the ones obtained from samples made by Ziegler–Natta catalysts, i.e. more comonomer content at the low MW end of the MWD. Moreover, both sample types have similar overall SCB distribution profiles across the MWD (i.e. slopes for the SCBD). However, these data suggest the presence of a SCB maximum not readily observed in samples made from the Ziegler–Natta catalyst.

Similarly, the TREF results of the two chromium-based samples in Fig. 3(b) exhibit a comonomer content composition distribution profile analogous to the one observed of the samples made by Ziegler–Natta catalysts. They are composed of a soluble fraction concentrated with comonomer content, a linear homopolymer fraction and an in-between, branched fraction of polymer molecules containing varying amount of comonomers. Also of note is the relative amount of the three constituent components of each individual sample varied in accordance with the density. The linear homopolymer fraction grows in its concentration

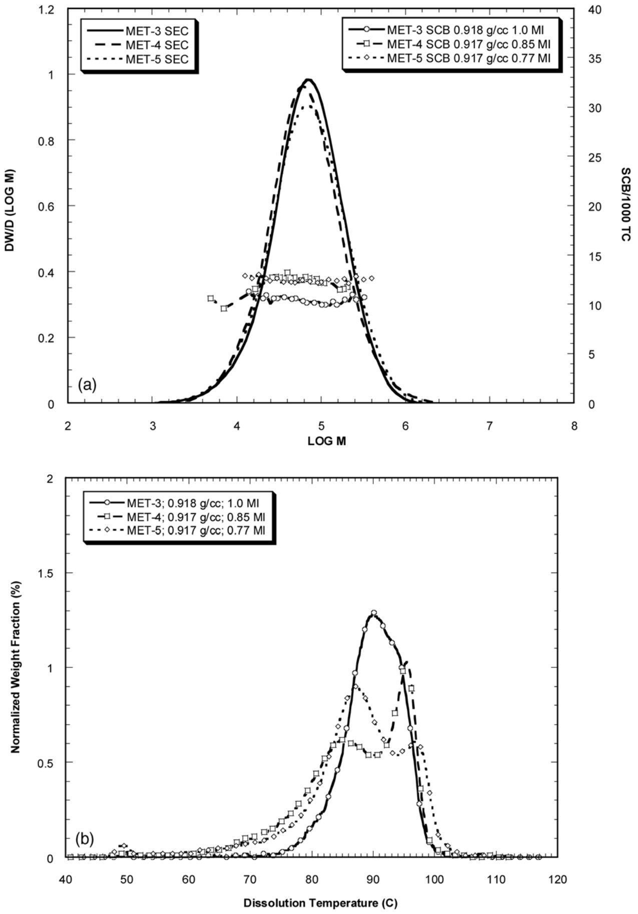

Fig. 4. (a) SEC-FTIR profiles of MET samples of comparable density. (b) TREF profiles of MET samples of comparable density.

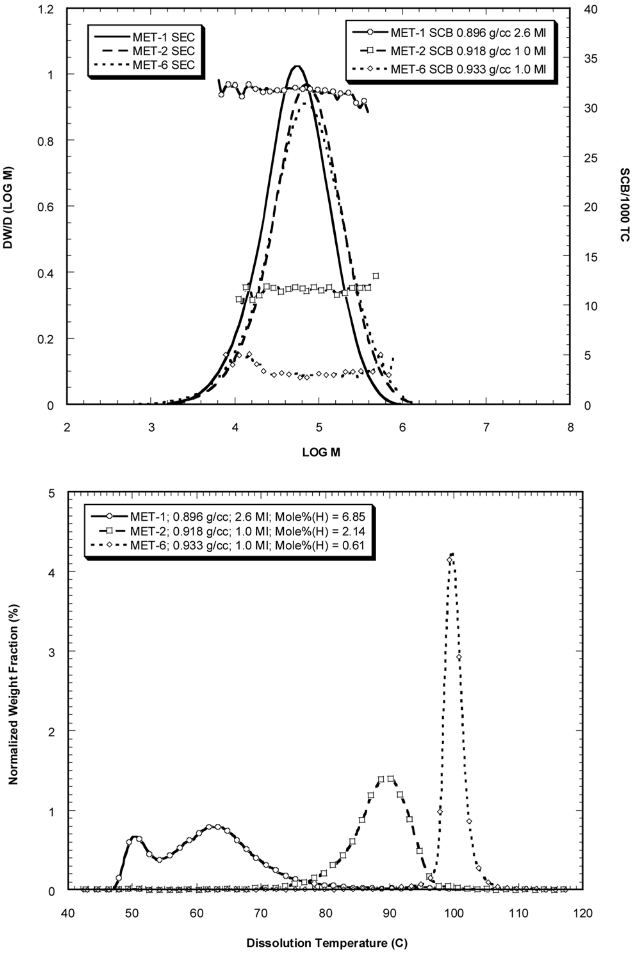

Fig. 5. (a) SEC-FTIR profiles of MET samples of different density. (b) TREF profiles of MET samples of different density.

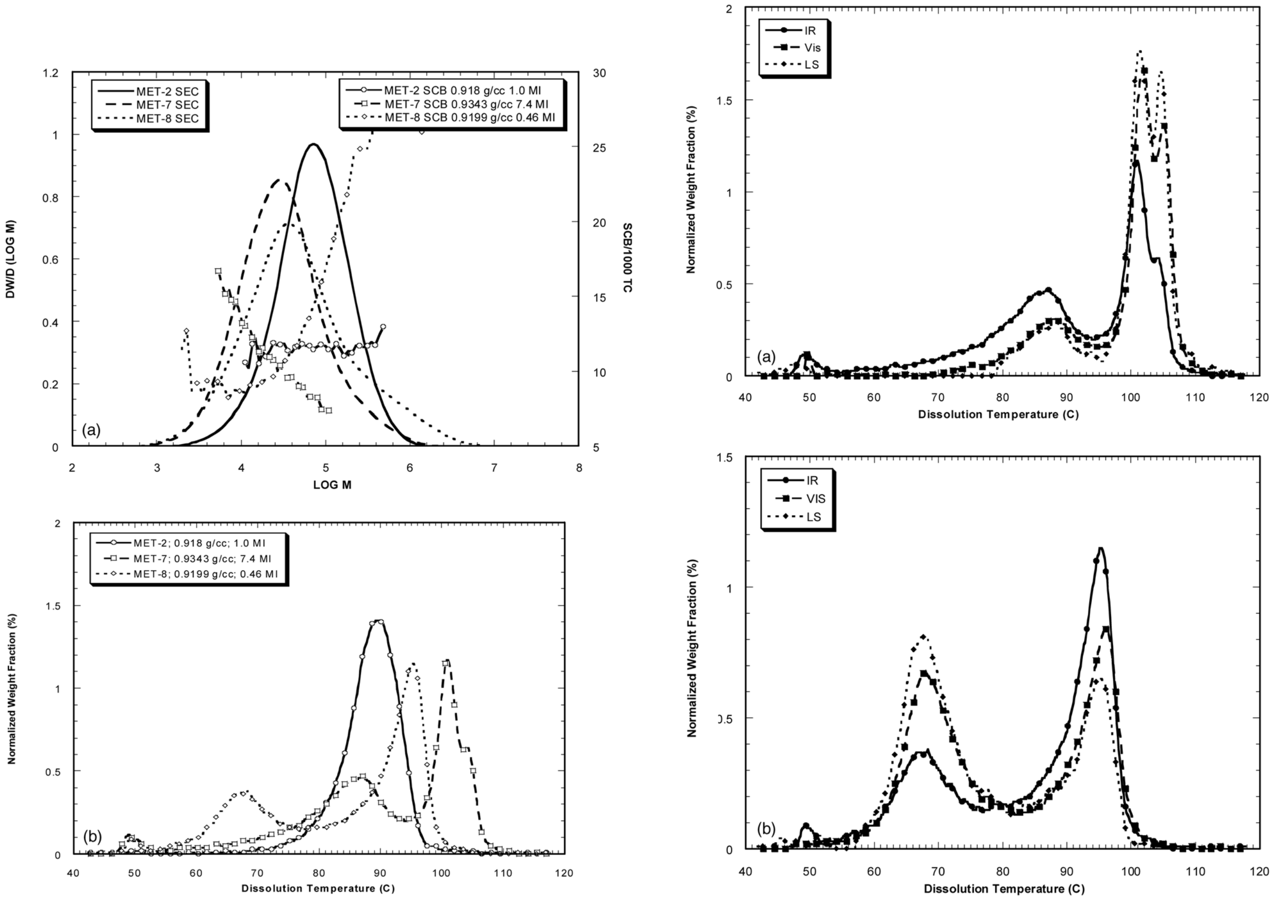

Fig. 6. (a) SEC-FTIR Profiles of samples by different MET catalysts. (b) TREF profiles of samples by different MET catalysts. (1) 3D-TREF profiles of sample MET-7. (2) 3D-TREF profiles of sample MET-8.

and the concentration of the soluble fraction goes in the opposite direction as the sample density increases.

3.3. Metallocene catalyzed resins

Fig. 4(a) shows the SEC-FTIR profiles of three copolymer samples of similar density produced by different metallocene catalysts. The profiles are all flat and sample MET-3 has lower comonomer content than the other two samples. This difference in comonomer content is also reflected in the ^{13}C NMR analysis of these samples. The corresponding TREF profiles for these samples (Fig. 4(b)) reveal noticeable differences, with sample MET-3 having the most homogeneous comonomer composition. These results also suggest a lower comonomer content for MET-3, which is consistent with both SEC-FTIR and ^{13}C NMR characterization of this resin.

Compared with the samples of similar density made from Ziegler–Natta catalysts, the constituent components of the metallocene samples have a much narrower range of the elution temperature as determined by 3D-TREF. These results suggest a more homogeneous comonomer content composition distribution profile. Furthermore, the metallocene samples contain very little, if any, soluble and the linear, homopolymer fractions as the Ziegler–Natta samples do.

Next, the SEC-FTIR profiles of three copolymer samples of different density produced by the same metallocene catalyst are shown in Fig. 5(a). The comonomer content distribution vs. MWD profiles are all fairly uniform and differ only in the overall comonomer content, which corresponds well with the resin density. Unlike the analogous Ziegler–Natta samples of varying density, the comonomers in the metallocene samples are not primarily located in the low MW end of the MWD, but instead, the comonomer is evenly incorporated across the MWD.

The corresponding TREF results for these samples are shown in Fig. 5(b). Clearly, the elution temperatures are distinctively different among the three samples, with the lower and higher density samples eluting out at lower and higher temperatures, respectively. Also of note is that the range of the elution temperature varies from broad to narrow as the density goes from low to high, indicating the comonomer composition distribution becomes more homogeneous as the density increases. These results are in stark contrast to what is observed for the samples produced by Ziegler–Natta catalysts, which show the same range of elution temperatures but varying in the relative amount of the three constituent fractions depending upon the density of the sample.

Fig. 6(a) shows the comonomer content distribution vs. MWD of three samples of similar density produced by different metallocene catalysts. First, in sample MET-2, a fairly uniform distribution profile could be seen. Secondly, sample MET-7 displays a distribution profile resembling the one observed of resins produced by Ziegler–Natta catalysts, i.e. higher comonomer content at the low MW end of the MWD. Lastly, sample MET-8 exhibits a profile trending in opposite direction to the one observed of sample MET-7, with more comonomer content concentrated at the high MW end of the MWD.

In the corresponding TREF profiles shown in Fig. 6(b), all three comonomer composition distribution profiles are also distinctively different from one another. Furthermore, the added viscometer and LS detectors give some MW-dependency information of the temperature fractions in these samples. Unquestionably, sample MET-2 has the most homogeneous distribution profile given its narrowest elution temperature range. Next, it is clearly seen that sample MET-7 has two major populations of polymer molecules of different comonomer content eluting out at separate temperatures. Comparing the relative peak heights between the IR, viscometer and LS detectors in Fig. 6b(1), the population of polymer molecules eluting out at higher temperature is definitely of higher MW and of lesser comonomer content by nature. Finally, sample MET-8 also displays two dominant populations of polymer molecules of different comonomer content and covers the broadest elution temperature range, which is indicative of its being most heterogeneous in its comonomer composition distribution profile. Contrary to sample MET-7, the population of polymer molecules coming out at lower elution temperature is of higher MW in Fig. 6b(2). Once again, the results from both SEC-FTIR and 3D-TREF methods are in agreement with one another. These results also clearly demonstrate that not all metallocene catalysts are single site catalysts.

3.4. Resin blends

It is obvious from the previous samples that one principal difference between 3D-TREF and SEC-FTIR is how these methods resolve compositional heterogeneity of samples that have similar molecular weights. This difference between the two methods is underscored when characterizing resin blends. The comonomer content for narrow MWD fractions obtained from the SEC-FTIR method is an average value of all polymeric molecules of varying comonomer content. The ability of SEC-FTIR analysis to discern a sample's compositional heterogeneity is dependent upon the extent to which the MWD of its components overlap. As the overlap between components increases, less compositional heterogeneity is detected. For example, Fig. 7(a) shows the SEC-FTIR profiles of a 50/50 blend sample, MET-9, and its two component resins, sample MET-2 and MET-6. Samples MET-2 and MET-6 have very similar MWs and MWDs. As expected, blend MET-9 exhibits an uniform comonomer content distribution vs. MWD profile and the overall comonomer content falling in between the two component resins. However, simply looking at the profile, there is no telling whether sample MET-9 is a blend or not.

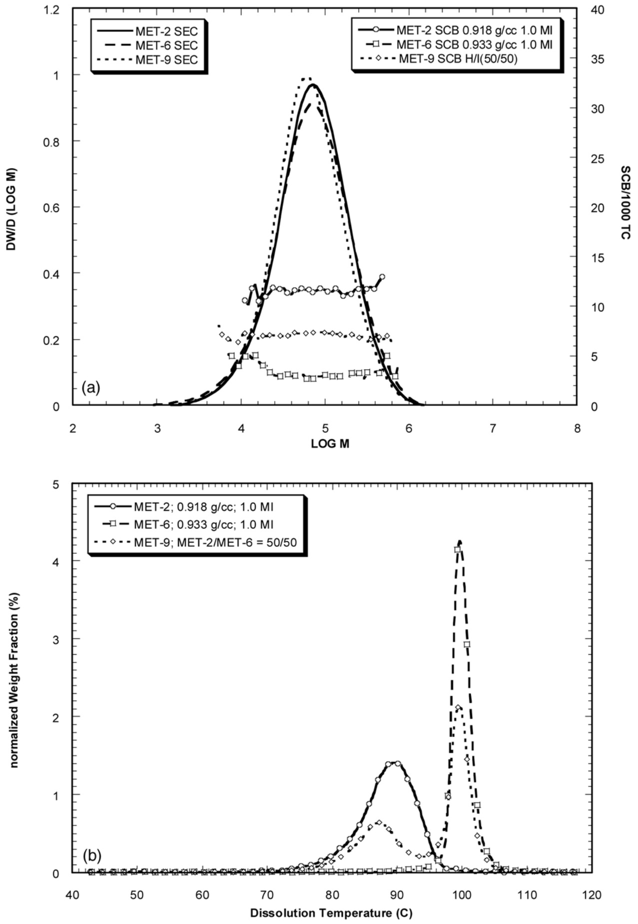

Fig. 7. (a) SEC-FTIR profiles of blend vs. component resins. (b) TREF profiles of blend vs. component resins.

By contrast, the corresponding TREF profile of the blend sample MET-9 in Fig. 7(b) clearly shows it is composed of two distinct populations of polymeric molecules of very different comonomer content. Compared with the profiles obtained from the individual component samples, MET-2 and MET-6, analyzed separately, no significant loss of resolution or shift in the elution temperatures is detected in the 3D-TREF analysis of the samples, MET-2 and MET-6, when run together in the blend MET-9. These results indicate there is minimal intermolecular interference during the crystallization or re-dissolution steps in the 3D-TREF method. However, we should note that 3D-TREF would have difficulty discriminating compositional heterogeneity in resin blends that are composed of two or more components with similar comonomer compositions, but with different molecular weights. For these latter types of resin blends, SEC-FTIR is the more appropriate method to detect compositional heterogeneity.

4. Conclusions

The SEC-FTIR method separates polymer molecules by their size and calculates the average comonomer content within each slice of narrow MWD via FTIR. The end product of this method is a comonomer content distribution vs. MWD profile. The salient feature of this method is that it reveals directly where the comonomers reside with reference to the MWD of the resin. The 3D-TREF method separates polymer molecules mainly by their crystallizability, which in turn is predominantly influenced by the comonomer content and its distribution within the molecules. This method yields a normalized distribution profile, of weight fraction vs. dissolution temperature, which reveals the comonomer composition of the resin. The spread of the temperature range and the variation of the weight fractions at different dissolution temperatures reflect the heterogeneity of the comonomer composition of the resin.

The two methods look at the resin molecular architecture from entirely different perspectives and complement each another. The choice of which method to use will be determined by the specific structure vs. property issue under study. Both methods are useful for characterizing LLDPE resins. However, the 3D-TREF method may offer more insight into the heterogeneity of resin blends, particularly when the blend components have similar molecular weights. Although some MW-dependency information of the temperature fractions can be ascertained via viscometer and LS detectors, SEC-FTIR is the more appropriate method to detect compositional heterogeneity in resin blends that are composed of two or more resins with the same copolymer compositions, but different molecular weights.

References

[1] Cady LD. Plast Engng 1987; January:25.
[2] Gabriel C, Lilge D. Polymer 2001;42:297.
[3] Faldi A, Soares JBP. Polymer 2001;42:3057.
[4] Verdurmen-Noel L, Baldo L, Bremmers S. Polymer 2001;42:5523.
[5] DesLauriers PJ, Rohlfing DC, Hsieh ET. Polymer 2002;43:159.
[6] Wild L, Ryle TR, Knobeloch DC, Peat IR. J Polym Sci, Phys Ed 1982; 20:441.
[7] Soares JBP, Hamielec AE. Polymer 1995;36:1639.
[8] Kelusky EC, Elston CT, Murray RE. Polym Engng Sci 1987;27:1562.
[9] Hosoda SJ. Polymer 1988;20:383.
[10] Defoor F, Groeninckx G, Schouterden P, Van der Heijden B. Polymer 1992;33:3878.
[11] Pigeon MG, Rudin A. J Appl Polym Sci 1994;51:303.
[12] Rudin A, Karbashewski E, Kale L, Tchir WJ. Polym Engng Sci 1993; 33:1370.
[13] Rudin A, Karbashewski E, Kale L, Tchir WJ, Schreiber HP. Polym Engng Sci 1991;31:1581.
[14] Zhang M, Llynch DT, Wanke SE. J Appl Polym Sci 2000;75:960.
[15] Zhang M, Lynch DT, Wanke SI. Polymer 2001;42:3067.
[16] Yau WW, Gillespie D, 2000 TAPPI Meeting.
[17] Yau WW, Gillespie D. Polymer 2001;42:8947.